Eur. Phys. J. D (2017) 71: 53
DOI: 10.1140/epjd/e2016-70583-8

THE EUROPEAN PHYSICAL JOURNAL D

Regular Article

Electron excited multiply charged argon ions studied by means of an energy resolved electron-ion coincidence technique

Sunil Kumar, Suman Prajapati, Bhupendra Singh, Bhartendu Kumar Singh, and Rama Shanker[a]

Atomic Physics Laboratory, Department of Physics, Institute of Science, Banaras Hindu University, 221005 Varanasi, India

Received 20 September 2016 / Received in final form 27 October 2016
Published online 7 March 2017 –

Abstract. Multiply charged argon ions produced from decay of L-shell hole states by impact of a *continuous beam* of 3.5 keV electrons are studied for the *first time* using an energy resolved electron-ion coincidence technique. The TOF spectra of argon ions are measured in coincidence with 18-energy selected electrons emitted in a wide energy range (126–242 eV). The coincidence measurement between the energy selected electrons and the correlated ions specifies the individual decay channel for various multiply charged ions. New experimental data are obtained and reported on the correlation probability for production of argon ions with charge states 1+ to 4+ as a function of ejected electrons in the considered energy range. The relative correlation probability of producing different charge state ions and corresponding physical processes involved in their production are presented and discussed. It has been found that the maximum probability for production of Ar^{2+} ions correlated to ejected Auger electrons in the energy range of 205–209 eV is 100%. No theoretical predictions are available to compare with these results. The present study shows further that not only the auto-ionization and normal Auger transitions but also several other decay processes including Coster-Kronig transitions followed by Auger cascades with a fraction of shake process play important role in producing ions with charge states 1+ to 4+.

1 Introduction

A number of measurements of multiply charged ions have been carried out through the photo-ionization of inner-orbital electrons of atoms [1–5] and through the electron impact ionization [6–11]. These multiply charged ions find wide applications in various fields of science and technology, for instance, fusion plasmas, ablation of surfaces by particle beams or lasers and in the analysis of space plasmas in the near earth environment and beyond. The ions formed by either photon or electron impact excitations usually originate through a cascade of transitions of electron emission in a non-radiative process. These transitions take place through the Coulomb interaction between the two electrons which take part in the normal or cascade Auger processes. In the normal Auger transition, the inner-shell hole is filled by the jump of one outer-shell electron whilst another outer-shell electron is ejected into the continuum. Also, electron-electron interaction may induce many particle effects including Auger shake-up and shake-off processes, in which a third electron from the outer- shell is excited to a discrete orbital or ejected into the continuum. Therefore, in order to understand and clarify the cascade mechanism in the production of multiply-charged ions, it is desirable to identify the kinetic energy of emitted electron responsible for each charge state of the ions. This identification would enable us to determine the intermediate state in the cascade decay pathways. This is possible by making use of a coincidence technique in which an energy selected electron and the correlated ion formed in the same event of collision are observed in coincidence. Such studies have been performed in the past by several workers mostly using the photo-ionization method to clarify the decay pathways, interference effects and the relative fractions of shake process, in the formation of multiply charged ions of rare gas atoms [12–19]. However, studies on formation of multiply charged rare gas atoms by impact of electrons using an energy selected electron-ion coincidence technique are limited to a small number, particularly, of argon atoms.

The early experiments to study the partial doubly differential cross sections for multiply charged ions of argon and other rare gas atoms by electron impact in the energy range of 0.5–28 keV employing the energy selected electron–ion coincidence experiments were performed by several workers [20–24]. Bučar and Zitnik [25] have performed the Auger electron-ion coincidence experiment by using a pulsed beam of 1 keV-electrons to study the argon L-MM Auger spectrum decomposing the contributions related to the specific final ionic charge states Ar^{2+} to Ar^{5+}. Their studies have shown the different decay schemes which lead to different structures in the non-coincidence Auger spectra.

The basic goal of the present work is to perform experiments using a continuous electron beam as ionising source. On one hand, Auger electron spectra (AES)

[a] e-mail: shankerorama@gmail.com

excited by keV-electrons are almost identical to the AES excited by white light [26]. On the other hand, electrons are able to produce auto-ionisation satellite lines (ASL) in the AES while a monochromotized light can produce ASL only for the proper selected values of the incident energies. In addition, the electron beam provides special advantage to make the electron-ion coincidence experiment more accessible due to the fact that a commercial (or home built) electron gun is easily available in most research laboratories and cheaper to use with respect to a synchrotron radiation source. The present study has been performed with an aim to shed further light in understanding the formation of multiply charged argon ions related to Ar L-shell hole cascade processes by means of an energy resolved electron-ion coincidence technique. Several experiments have been carried out on studies of multiple ionization of argon atom using coincidences between electrons of unselected energy and produced ions by impact of either a continuous or a pulsed beam of energetic electrons, see for example, Okudaira et al. [8], Krishnakumar and Srivastava [27], Ma et al. [28], McCallion et al. [29], Almeida et al. [30] and references therein; likewise, a number of experiments have been performed on the study of multiple ionization of argon atom using Auger electron-ion coincidence technique through photo-ionization, for instance, Brünken et al. [31], von Busch et al. [32], Alkemper et al. [33], Ricz et al. [34] and others. The detail theoretical and experimental study on the $2s$ and $2p$ hole decay of argon and formation of multiply charged ions has been reported by Lablanque et al. [35,36]. However, to the best of author's knowledge, the present work on identification of different decay pathways of Ar L-shell hole states and on correlation probability for production of multiply charged argon ions as a function of ejected electron energy under impact of a *continuous* beam of keV-electrons is reported *for the first time*. The results derived from the present measurements are expected to yield supplementary information towards a comprehensive test of the calculations.

2 Experimental method

Experiments were carried out on our recently developed set up for studying the collision induced processes by energetic charged particles (electrons and ions) with atomic, molecular and solid targets. For the present studies, the set up has consisted of a mono-energetic source of electrons (PSP Model: ELS-5000, UK), a home built double field type of time of flight (TOF) mass spectrometer [37] and a single pass cylindrical mirror analyser (CMA) (PHI-Model No.15-110A). The CMA has an angular acceptance of $\pm 7°$ around the mean acceptance angle of about 43°. Its geometrical solid angle $\Delta\Omega$ is determined to be about 8.4% of 4π. Two spectrometers are set in opposite directions and the detection axes of these spectrometers are orthogonal to both the electron beam and the gas injection direction. Figure 1 shows a schematic diagram of a system for measuring the TOF spectra where the electron impact excited multiply charged argon ions are observed in coincidence with different values of energy selected electrons.

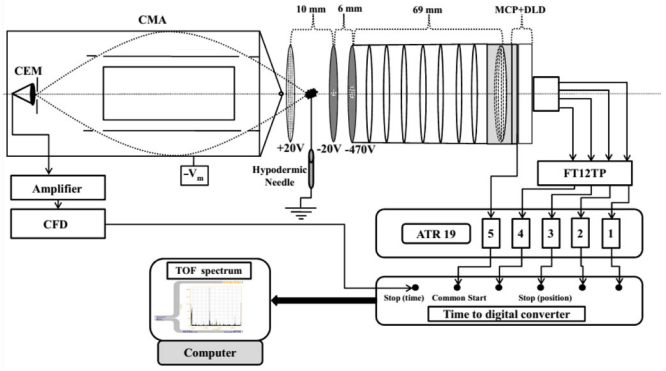

Fig. 1. Auger electron-ion coincidence measurement system using a double field TOF mass spectrometer and a single-pass cylindrical mirror analyser (CMA). FT12-TP: RC decoupling unit, ATR: fast differential amplifier with constant fraction discriminator modules, CEM: channel electron multiplier. For explanation of different components of the system, see text.

The mono-energetic electron beam crosses the sample gas (argon) beam which effuses from a grounded hypodermic needle (i.d. = 1 mm and length = 30 mm) at a right angle. A static electric field of 40 V cm^{-1} was symmetrically applied to the ionization region during the coincidence measurements. The diameter of the electron beam at the scattering centre is about 1.0 mm. This corresponds to an indetermination of 4.0 eV in the Auger electron energy when the above static electric field is applied to the interaction region.

The collision induced Ar^{n+} ions (n = 1–4) were extracted in the opposite direction to the electrons, analysed their charge states by a TOF mass spectrometer and detected by a dual micro-channel plate (MCP) detector of diameter 40 mm equipped with a delay line anode detector (DLD) assembly [38]. During the coincidence measurements, the pass energy of the CMA was fixed at selected electron energy. The signal from the MCP is taken as START pulse while the signal from the CMA is taken as the STOP pulse. Both the signals are then fed to the time-to-digital converter (TDC) operated in a multi-hit configuration to obtain coincidence TOF spectra (Fig. 1). The digitized data obtained from the TDC are stored in a list mode for each event on a hard disk. The Cobold PC software is used for data acquisition and off-line analysis. The background pressure of the scattering chamber was 9×10^{-7} Torr while the pressure of the chamber with gas load was maintained at 5×10^{-5} Torr. The argon gas (stated purity 99.9%) used in this study was purchased from M/s Inox Air Production, India. The measured electron energy resolution $\Delta E/E$ of the CMA was determined to be 2.5%. This value is mainly controlled by the size of interaction zone which in the present case is about 1 mm × 1 mm. With such an intrinsic energy resolution, the presence of a dc field (40 V cm^{-1}) in the interaction region neither worsens the energy resolution of the electron energy spectra measured by the CMA nor deflects the electron beam in the interaction region. From an auxiliary experiment, it has been verified that with and without the applied static field, the electron spectrum remains

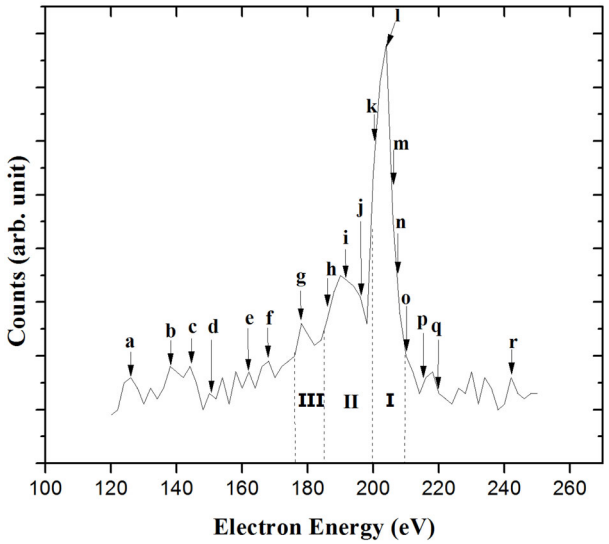

Fig. 2. Electron energy spectrum of argon produced by impact of 3.5 keV electrons with a dilute argon gas target in the ejected electron energy range of 120–250 eV in presence of 40 V cm^{-1} electric field applied in the gas-beam interaction region. Arrows below alphabetical symbols denote the energy positions where the coincidence measurements were performed. The dotted vertical lines separate the three main groups I, II and III of the Auger transition lines of considerable intensities (see, text).

identical in relation to its shape, resolution and energy distributions. With a typical electron beam current of 20 pA, the count rates of detected ions and of known energy electrons were 60 kHz and 4–5 Hz respectively. Under such conditions, the data accumulation time of about 25–30 h for each electron-ion coincidence spectra was needed. More details of the experimental set-up, the detector signals processing and that of the data acquisition procedures will be given elsewhere.

3 Results and discussion

3.1 Electron energy spectrum

Figure 2 shows an electron energy spectrum of argon produced by impact of 3.5 keV electrons with a dilute argon gas target in the ejected electron energy range of 120–250 eV. The spectrum was measured with 40 V cm^{-1} electric field applied in the electron beam-gas interaction region. The kinetic energy of electrons measured in the CMA was calibrated by the peak energy of L_{23}-M_{23} M_{23} ($^1D_2$) Auger transition occurring at 203.5 eV [37]. A group of multiple peaks (group I) with highest intensity around 203.5 eV arises from the decay of L_{23}-M_{23} M_{23} Auger transitions. The structure around 192 eV forms the group II due to L_3-M_1 M_{23} ($^1P_1$, $^3P_{2,1,0}$) transitions and the structure around 178 eV (group III) corresponds to L_{23}-M_1 M_1 ($^1S_0$) transitions. Small structures below 178 eV and above 210 eV are also seen which are ascribed to arise from different decay channels giving rise

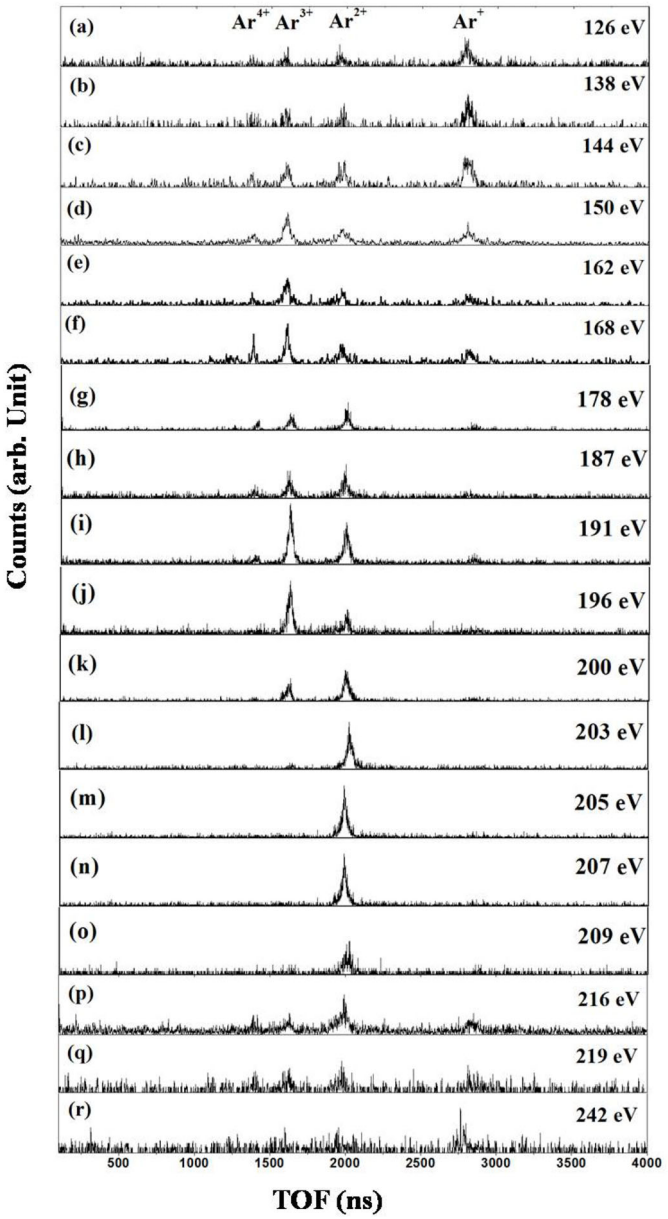

Fig. 3. TOF spectra of multiply charged argon ions observed in coincidence with 18-energy selected electrons shown in panels (a)–(r). The energy values listed on the right hand side denote those of electrons selected with the electron energy analyser. The data collection time of each spectrum ranged from 25 to 30 h.

to a variety of final ion charge states with weak intensities (as observed in the electron-ion coincidence spectra, see Fig. 3). Following Werme et al. [39], group I of the Auger transition lines is found to consist of four (presently unresolved) major diagram lines, namely, L_{23}-M_{23} M_{23} ($^1D_2$) at 203.5 eV, L_3-M_{23} M_{23} ($^1S_0$) at 201.1 eV, L_3-M_{23} M_{23} ($^3P_{2,1,0}$) at 205.2 eV and L_2-M_{23} M_{23} ($^1D_2$) at 205.6 eV. The group II comprises of two unresolved Auger diagram lines, namely, L_3-M_1 M_2 ($^3P_{2,1,0}$) at 191.0 eV and L_3-M_1 M_{23} ($^1P_1$) at 189.0 eV. The group III contains unresolved weak lines of Auger transitions, namely, L_3-M_1M_1 ($^1S_0$)

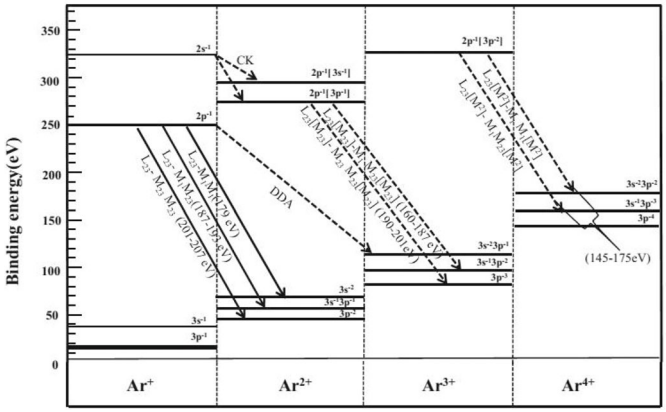

Fig. 4. Energy level diagram of argon ions and different transition channels. The horizontal solid lines denote the energy levels obtained from Lotz [40] and Larkins [41]. Solid arrows indicate diagram lines of Auger transitions whereas the dotted ones denote Coster-Kronig (CK) combined with Auger transitions leading to satellite lines. The predicted energy regions of various satellite transitions are shown in brackets for each decay channels. Contribution is shown for direct double Auger (DDA) process to produce Ar^{3+} ions following transitions from $2p^{-1}$ to $(3s^{-2}3p^{-1})$ [31].

at 177.9 eV, L_3-M_1M_{23} ($^1P_1$) at 179.0 eV and L_3-M_1M_{23} ($^3P_{0,1,2}$) at 179.5 eV. We have measured the coincidences of multiply charged argon ions with 18-energy selected electrons (see arrows indicating below alphabets (a) to (r) in Fig. 2). These measurements provide the detailed information about the nature of multiply charged argon ions formed due to decay of L-shell hole states of argon at the considered impact energy of electrons.

3.2 Ion coincidence spectra with energy selected electrons

The argon ion coincidence TOF spectra have been recorded with impact of 3.5 keV electrons for a whole series of 18-pass energies of electron spectrometer at an effective energy resolution of about 5eV. The observed ion coincidence TOF spectra are displayed in Figure 3.

The selected electron energies are indicated on the right hand side of each panel in order of the kinetic energy of the detected electrons. These spectra contain several charge states of ions which indicate that the charge number of argon ions increases with the decrease in electron energy. This also means that the charge number of ions increases with increase in final state energy.

A schematic diagram of energy levels of Ar^{n+} ions (n = 1–4) together with different decay channels is shown in Figure 4.

The binding energies of electrons in different sub-shells of argon ions of charge states 1+ to 4+ relevant to L-MM Auger transitions are taken from the work of Lotz [40] which are shown by the horizontal solid lines. Very similar values of binding energies of all considered sub-shells are also obtained from the 'adiabatic' model of Larkins [41] wherein the time of Auger transitions (10^{-14}–10^{-15} s) is comparable or more to the life-time of a vacancy in the atom ($\sim 10^{-15}$ s); this condition is expected to prevail in our experiments suggesting that during the Auger transitions, the ionized atom may undergo the shake-up and shake-off processes. In Figure 4, the slanted solid line arrows indicate the observed normal Auger transitions whereas the dashed ones show the successive Auger decay channels giving rise to different satellite lines. The latter ones are inferred from the electron-ion coincidence measurements. Various Auger decay channels obtained from electron-ion coincidence measurements are discussed in the following lines.

The ion coincidence TOF spectra shown in panels (a)–(f) of Figure 3 for electrons having energy in the range of 126–168 eV are seen to possess a common feature, that is, each one of them exhibits argon ion charge states from 1+ to 4+. The Ar^+ peaks for electron energies at 126 eV, 138 eV, and at 144 eV are found to have similar intensity whereas the intensity of this peak reduces gradually to zero in going from 150–178 eV. Specifically, those Ar^+ ions which are formed in energy region 126–168 eV are ascribed to originate from the post collision interaction (PCI) in which the ejected electrons from Auger process are captured by Ar^{2+} ions resulting into Ar^+ [42].

The spectra shown in Figures 3d–3f exhibit the Ar^{3+} satellite peaks slightly more intense than those present in Figures 3a–3c. The selected electrons of energy 150–168 eV are assumed to correlate with Ar^{2+} with final states $3s^{-1}3p^{-1}$ (M_1M_{23}). These ions finally turn into Ar^{3+} ($3p^{-3}$) by a subsequent electron emission through the CK transitions [43]. Further, it may be mentioned that the Ar^{3+} ions correlated to electrons having energy 140–170 eV are known to be formed through direct double Auger (DDA) process via transitions of type $2p^{-1} - 3s^{-2}3p^{-1}$, $2p^{-1} - 3p^{-3}$ [31] (see, Fig. 4).

The spectra contained in panels (g)–(k) of Figure 3 are seen to exhibit only two strong peaks namely, Ar^{2+} and Ar^{3+} (and very weak Ar^{4+}) at each Auger electron energy in the range 178–200 eV. The existence of these peaks in this energy range is understood by the fact that all major Auger transitions, namely, Auger final states are $3s^{-1}3p^{-1}$ ($^1P_1$, $^3P_{012}$) with transitions L_{23}-M_1M_{23} in the energy range of 187–193 eV; the Auger transition line ($^1P_1$) lying at 187 eV and $^3P_2$ line around 191 eV are found to be the prominent transition lines in this energy range both of which correlate to Ar^{2+} ions [39]. However, the peak appearing at 191 eV also correlates to Ar^{3+} ions occurring due to L_{23}-[M_{23}]-$M_{23}M_{23}$[M_{23}] transition (see, Fig. 4) where [M_{23}] refers to a spectator vacancy and L_{23}-$M_{23}M_{23}$ ($^1D_2$) at 203 eV; L_{23}-M_1M_{23} ($^1P_1$) at 187 eV and L_3-$M_{23}M_{23}$ ($^3P_2$) at 191 eV occur to yield Ar^{2+}. The Ar^{3+} and Ar^{4+} ions are produced following the Auger cascade transitions with spectator vacancies [M_{23}] of the type: L_{23} [M_{23}]-$M_{23}M_{23}$[M_{23}] and L_{23} [M_{23}]^2-$M_{23}M_{23}$[M_{23}]^2 falling in the range 190–201 eV [43].

The only Ar^{2+} peaks observed at Auger electron energies in the range 203–209 eV are shown in panels (l)–(o) of Figure 3. These peaks are produced due to main Auger

transitions, namely, L_3-$M_{23}M_{23}$ ($^1D_2$) at 203.5 eV, L_3-M_{23} M_{23} ($^3P_{2,1,0}$) at 205.2 eV and L_2-$M_{23}M_{23}$ ($^3P_{2,1,0}$) at 207.2 eV [39]. These peaks are not resolved and appear single in our electron energy spectrum due to insufficient resolution of the present electron analyzer (see, Fig. 2). All transitions are known to produce Ar^{2+} ions only.

The spectra presented in Figures 3p–3r correspond to electrons having energy in the range of 216–242 eV. These coincidence spectra show weak structures of argon ion peaks of charge states 1+ to 4+ with poor count statistics. The formation of Ar^+ ions appearing in energy range 216–242 eV can take place through different processes, for instance, (i) the direct ionization; (ii) the excitation of $2p$ sub-shell electrons into a discrete energy level with the subsequent Auger decay of the $2p$-vacancy and ejection of a fast electron; (iii) ionization of a $2p$ sub-shell electron with its subsequent capture into a discrete level of the remaining ion, which is rearranged after the $2p$-vacancy Auger decay in which a fast electron leaves the atom [44]. The production of Ar^{2+}, Ar^{3+} and Ar^{4+} ion peaks in this energy range is assumed to take place through different possible reaction processes, namely, (i) presence of multiple spectator vacancies created by CK transitions in the initial channel and subsequently filled through Auger transitions [43]; (ii) double Auger transitions, shake-up and shake-off processes [45] and resonant Auger transitions [46].

The results obtained in the present work indicate that not only the normal Auger and auto-ionization processes but also several other processes (CK transitions, DDA, resonant Auger transitions, PCI and shake processes) followed by Auger cascades with multiple spectator vacancies are responsible to produce multiply charged argon ions formed in coincidence with different energy selected electrons due to decay of L-shell hole states of Ar atom. As shown in Figure 2, the most probable decay process in the initial step is the Auger electron emission of L_{23}-$M_{23}M_{23}$ ($^1S_0$, $^1D_2$, $^3P_{2,1,0}$) in the energy range 200–210 eV. The second most probable one is that of the L_{23}-M_1M_{23} ($^3P_{2,1,0}$, $^1P_1$) in the energy range of 185–200 eV. The third probable decay process corresponds to the Auger satellite transitions in the electron emission range of 170–185 eV. Thus, it can be concluded that a significantly high fraction of the finally formed multiply charged argon ions are produced through the pathway into the highest state between all energetically possible states from the Auger final states.

The coincidence spectra presented in Figure 3 do not show distinctly the formation of Ar^{5+} ions although their signatures are visible (see, Fig. 3d and 3f). This observation indicates that a fraction of shake-off process may be effective to produce these ions. This finding suggests that these ions are not formed through the normal Auger transitions; probably, they are formed through initial Auger shake process which forms highly charged ions positioned at energy levels higher than the ground state of Ar^{5+}.

The present findings on the production of multiply charged argon ions obtained from our coincidence experiments are represented by the following decay routes which lead to different charge states of the argon ions:

$$\mathrm{Ar}^+(2p^{-1}) \rightarrow \mathrm{Ar}^{2+}(3p^{-2}) \text{ via } \mathrm{L}_{23} - \mathrm{M}_{23}\mathrm{M}_{23} \quad (1)$$

$$\rightarrow \mathrm{Ar}^{2+}(3s^{-1}, 3p^{-1}) \text{ via } \mathrm{L}_{23} - \mathrm{M}_1\mathrm{M}_{23} \quad (2)$$

$$\rightarrow \mathrm{Ar}^{2+}(2p^{-1}, 3p^{-1}) \rightarrow (3p^{-2}[3p^{-1}])$$
$$\text{via } \mathrm{L}_{23}[\mathrm{M}_{23}] - \mathrm{M}_{23}\mathrm{M}_{23}[\mathrm{M}_{23}] \rightarrow \mathrm{Ar}^{3+} \quad (3)$$

$$\rightarrow \mathrm{Ar}^{2+}(2p^{-1}, 3p^{-1}) \rightarrow (3s^{-1}3p^{-1}[3p^{-1}])$$
$$\text{via } \mathrm{L}_{23}[\mathrm{M}_{23}] - \mathrm{M}_1\mathrm{M}_{23}[\mathrm{M}_{23}] \rightarrow \mathrm{Ar}^{3+} \quad (4)$$

$$\rightarrow \mathrm{Ar}^{2+}(2p^{-1}, 3p^{-1}) \rightarrow (3s^{-2}[3p^{-1}])$$
$$\text{via } \mathrm{L}_{23}[\mathrm{M}_{23}] - \mathrm{M}_1\mathrm{M}_1[\mathrm{M}_{23}] \rightarrow \mathrm{Ar}^{3+} \quad (5)$$

$$\rightarrow \mathrm{Ar}^{3+}(2p^{-1}3p^{-2}) \rightarrow (3p^{-2}[3d^{-2}])$$
$$\text{via } \mathrm{L}_{23}[\mathrm{M}^2] - \mathrm{M}_1\mathrm{M}_1[\mathrm{M}^2] \rightarrow \mathrm{Ar}^{4+} \quad (6)$$

$$\rightarrow \mathrm{Ar}^{3+}(2p^{-1}3p^{-2}) \rightarrow (3s^{-1}3p^{-1}[3d^2])$$
$$\text{via } \mathrm{L}_{23}[\mathrm{M}^2] - \mathrm{M}_1\mathrm{M}_{23}[\mathrm{M}^2] \rightarrow \mathrm{Ar}^{4+} \quad (7)$$

$$\mathrm{Ar}^+(2s^{-1}) \rightarrow \mathrm{Ar}^{2+}(3s^{-2})$$
$$\text{via } \mathrm{L}_1 - \mathrm{L}_{23} \rightarrow \mathrm{L}_{23} - \mathrm{M}_1\mathrm{M}_1 \rightarrow \mathrm{Ar}^{2+} \quad (8)$$

$$\rightarrow \mathrm{Ar}^{3+}(3s^{-2}3p^{-1})$$
$$\text{via } \mathrm{L}_1 - \mathrm{L}_{23}[\mathrm{M}] \rightarrow \mathrm{L}_{23} - \mathrm{M}_1\mathrm{M}_1[\mathrm{M}] \rightarrow \mathrm{Ar}^{3+} \quad (9)$$

$$\rightarrow \mathrm{Ar}^{3+}(3s, 3p)^{-3}$$
$$\text{via } \mathrm{L}_1 - \mathrm{L}_{23}[\mathrm{M}^2] \rightarrow \mathrm{L}_{23}[\mathrm{M}^2] - \mathrm{M}_1\mathrm{M}_{23}[\mathrm{M}^2] \rightarrow \mathrm{Ar}^{4+}. \quad (10)$$

The results obtained in this work indicate that the normal Auger combined with other different processes produce ions in the charge states of 1+ to 4+ due to decay of the L-shell hole states of the argon atom. Intensity variation of lines arising due to different decay pathways depends mainly on whether the initial state has a spectator vacancy (represented by states in square brackets). Such states usually give rise to a satellite line. Normally, the intensity of satellite transition lines (Eqs. (3)–(7)) is found to be weaker than the intensity of diagram lines (Eqs. (1)–(2)). The role of CK transitions can be visualized from equations (8)–(10) for production of argon ions of charge states 3+ and 4+. In these cases, the initial vacancy is created in $2s$ (L_1) sub-shell which is filled by L_{23} sub-shells electron and emitting an electron from M_{23} sub-shell resulting into two vacancies: one in L_{23} and other in [M_{23}] sub-shell as a spectator vacancy; subsequently the L_{23} vacancy is filled through the Auger transitions yielding one higher ionic charge state of the atom (see, Eq. (9)).

3.3 Relative correlation probability

We have studied the relative correlation probabilities of Ar^{n+} ions (n = 1–4) as a function of energy of ejected

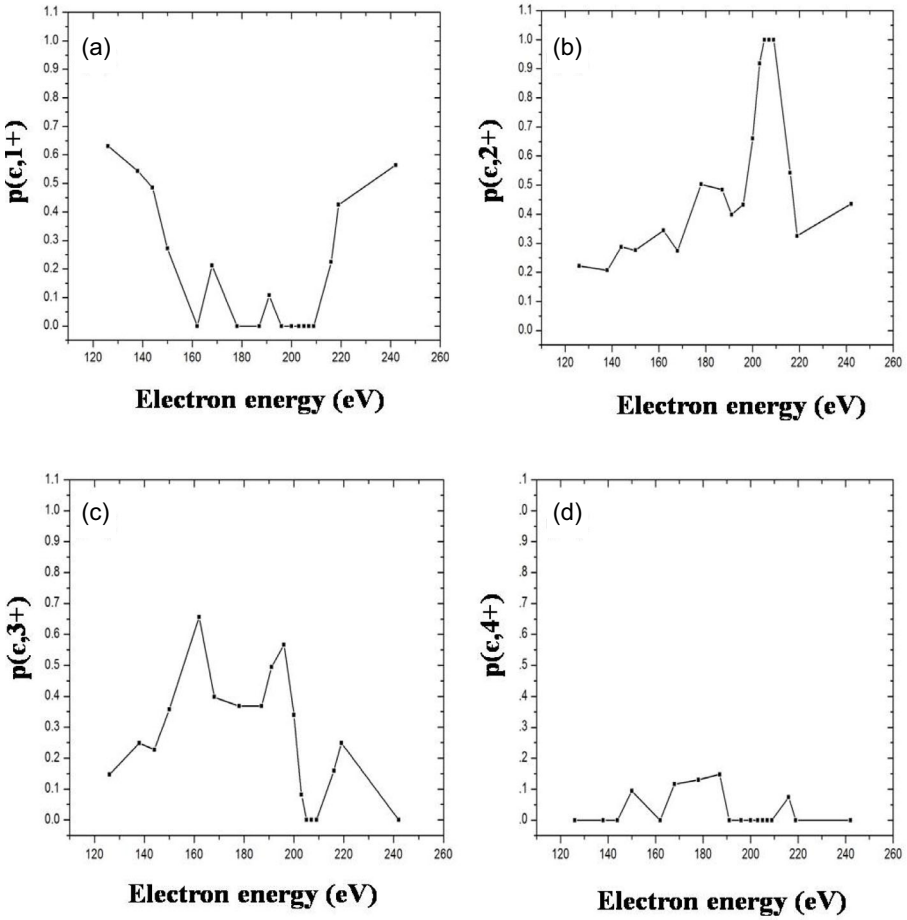

Fig. 5. Relative correlation probability $p(\varepsilon, n+)$ for production of argon ions with charge states 1+ to 4+ as a function of electron energy ε. (a) Ar^{+}, (b) Ar^{2+}, (c) Ar^{3+} and (D) Ar^{4+}. For explanation, see text.

electrons. In this study, we have determined the probability $P(nl^{-1}, n+)$ for the decay of an inner-shell hole state nl^{-1} (initial state) into different ionic charge states $n+$ (final state). The correlation probability $p(\varepsilon, n+)$ thus measured at a kinetic energy ε of a specific ejected electron which corresponds to the initial state for a final charge state $n+$ of the ion provides information on the decomposition of electron spectrum that correlates the electron impact ionization processes ending up in a certain final ionic charge state. In order to obtain the correlation probabilities $p(\varepsilon, n+)$ from the ion-coincidence TOF spectra for each coincidence measurements at kinetic energy ε, the sum $\sum_{n=1} p(\varepsilon,\ n+)$ is normalize to 1. As a result, we obtain the values of $p(\varepsilon, n+)$ for the given final charge state $n+$ at each electron energy ε. Such results have been obtained and displayed in Figure 5 for argon ions with charge states 1+ to 4+.

The distributions of Ar^{+} ions presented in Figure 5a show the probability of production of Ar^{+} ions as a function of emitted electron energy ε. It is seen that this probability attains a value of 63% at $\varepsilon = 126$ eV but it decreases gradually to 0% at $\varepsilon = 178$ eV. A reverse trend is noted wherein $p(\varepsilon, 1+)$ rises from 0% at $\varepsilon = 216$ eV and reaches maximum of about 56% at $\varepsilon = 242$ eV. However, the yield of Ar^{+} ions is seen to be about 20% at electron energy of 168 eV and about 10% at 191 eV; these ions are produced due to the contribution of direct ionisation of valence electrons. The decrease of Ar^{+} ions in the energy range 160–210 eV corresponds to increase in yields of Ar^{2+} ions (see, Fig. 5b). The present analysis concludes that Ar^{+} ions attain maximum probability of their production corresponding to emission of low energy electron at $\varepsilon = 126$ eV and to emission of high energy electrons at $\varepsilon = 242$ eV in the present experimental conditions.

The spectrum presented in Figure 5b exhibits the correlation probability for production of Ar^{2+} final charge state as a function of ε. This distribution shows that there is 100% probability of Ar^{2+} ion production corresponding to emission of Auger electrons having energy in the range of 205–209 eV. However, the correlation probability assumes values of 32–43% for production of Ar^{2+} ions in the electron emission energy range of 219–242 eV and 22–43% in the energy range of 126–196 eV.

The graph shown in Figure 5c presents the correlation probability of Ar^{3+} ions production as a function of emission energy of electrons in the considered collision system. Here, we see that about 50% of these ions are correlated to the ejected electrons of 190 eV energy while about 46% are corresponding to electrons of 160 eV energy. The correlation probability reduces from 46% to about 15–25%

for electrons having energy in the range of 216–230 eV respectively. About 20% probability of Ar^{3+} ion production is found for electron energy of 220 eV.

Figure 5d exhibits the graph for correlation probability versus ejected electron energy ϵ for production of Ar^{4+} ions in collision of 3.5 keV electrons with neutral argon atoms. It is seen that the production probability of Ar^{4+} ions correlated to the ejected electrons of energies 150–191 eV amounts to only 10–20% maximum while no Ar^{4+} ions are produced with correlated ejected electrons having energy between 190–210 eV and 219–242 eV; however, there is a small probability of about 7% of their production for correlated electrons with energy of about 216 eV.

The above analysis on the correlation probability for production of argon ions with charge states 1+ to 4+ shows clearly that the maximum probability of 100% is found for production of Ar^{2+} ions correlated to ejected Auger electrons with energy in the range of 205–209 eV; in this region most intense diagram lines of Auger transitions are found to occur (see, Sect. 3.1).

4 Conclusions

The TOF spectra of argon ions induced by impact of a continuous beam of 3.5 keV electrons with argon atoms have been studied in coincidence with 18-energy selected electrons which are emitted from the target atoms in energy range of 126–242 eV. From the analysis of these spectra, it is found that the production of Ar^{+} ions decreases gradually from its maximum value of 63% to 0% having correlation with the ejected electrons of energy from 126 eV to 162 eV respectively; less than 10% Ar^{+} ions are seen to make their presence in the electron energy range from 178 eV to 209 eV. The production probability of these ions further rises from 0% at 209 eV and reaches maximum of 56% at 242 eV. The correlation probability for production of argon ions with charge states 1+ to 4+ as a function of electron energy shows that the maximum probability of 100% is found for production of Ar^{2+} ions correlated to ejected Auger electrons with energy in the range of 205–209 eV. In summary, the present study has shown that not only the normal Auger and auto-ionization transitions but also CK transitions, DDA, PCI, resonant Auger and shake processes followed by Auger cascades play important role in producing ions with charge states 1+ to 4+ due to decay of L-shell hole states of argon atom under impact of the considered energetic electrons. It is thus concluded that a significantly high fraction of finally formed multiply charged argon ions are produced through subsequent successive various decay pathways.

This work has been supported in part by the Department of Science and Technology (DST), New Delhi, Government of India. A significant part of the development of the experimental set up has been executed under support from the Board of Research in Fusion Science and Technology (BRFST), Institute for Plasma Research (IPR), Ahmedabad, under the Department of Atomic Energy (DAE), Government of India. We would like to thank Pragya Bhatt, Raj Singh and Namita Yadav for their continuous support and help in the initial phase of development of the employed experimental set up.

References

1. M.O. Krause, T.A. Carlson, Phys. Rev. **158**, 18 (1967)
2. T. Tonuma, A. Yagishita, H. Shibata, T. Koizumi, T. Matsuo, K. Shima, T. Mukoyama, H. Tawara, J. Phys. B **20**, L31 (1987)
3. Y. Tamenori, K. Okada, S. Nagaoka, T. Ibuki, S. Tanimoto, Y. Shimizu, A. Fujii, Y. Haga, H. Yoshida, H. Ohashi, I.H. Suzuki, J. Phys. B **35**, 314 (2002)
4. N. Saito, I.H. Suzuki, J. Phys. B **25**, 1785 (1992)
5. T.A. Carlson, W.E. Hunt, M.O. Krause, Phys. Rev. **151**, 41 (1966)
6. B. Adamczyk, J. Chem. Phys. **44**, 4640 (1966)
7. M.J. van der Wiel, T.M. El-Sherbini, L. Vriens, Physica **42**, 411 (1969)
8. S. Okudaira, Y. Kaneko, I. Kanomata, J. Phys. Soc. Jpn **28**, 1536 (1970)
9. T.M. El-Sherbini, M.J. Van der Wiel, F.J. de Heer, Physica **48**, 157 (1970)
10. R.K. Singh, R. Shanker, J. Phys. B **36**, 1545 (2003)
11. S. Mondal, R. Shanker, Phys. Rev. A **72**, 052705 (2005)
12. N. Saito, I.H. Suzuki, J. Electron Spectrosc. Relat. Phenomena **88-91**, 65 (1998)
13. J.C. Levin, C. Biedermann, N. Keller, L. Liljeby, C.-S. O, R.T. Short, I.A. Sellin, D.W. Lindle, Phys. Rev. Lett. **65**, 988 (1990)
14. W. Eberhardt, S. Bernstorff, H.W. Jochims, S.B. Whitfield, B. Crasemann, Phys. Rev. A **38**, 3808 (1988)
15. G. Armen, J. Levin, I. Sellin, Phys. Rev. A **53**, 772 (1996)
16. D.V. Morgan, M. Sagurton, R.J. Bartlett, Phys. Rev. A **55**, 1113 (1997)
17. N. Saito, I.H. Suzuki, J. Phys. Soc. Jpn **66**, 1979 (1997)
18. B. Kammerling, B. Krassig, V. Schmidt, J. Phys. B **25**, 3621 (1992)
19. E. Shigemasa, T. Koizumi, Y. Itoh, T. Hayaishi, K. Okuno, A. Danjo, Y. Sato, A. Yagishita, Rev. Sci. Instrum. **63**, 1505 (1992)
20. R. Hippler, K. Saeed, A.J. Dumcan, H. Kleinpoppen, Phys. Rev. A **30**, 3328 (1984)
21. R.K. Singh, R. Hippler, R. Shanker, J. Phys. B **35**, 3243 (2002)
22. M.A. Chaudhry, A.J. Duncan, R. Hippler, H. Kleinpoppen, Phys. Rev. A **39**, 530 (1989)
23. R.K. Singh, S. Mondal, R. Shanker, J. Phys. B **36**, 489 (2003)
24. S. Mondal, R. Shanker, Phys. Rev. A **72**, 062721 (2005)
25. K. Bučar, M. Žitnik, Rad. Phys. Chem. **76**, 487 (2007)
26. H. Sambe, D.E. Ramaker, Chem. Phys. Lett. **128**, 113 (1986)
27. E. Krishnakumar, S.K. Srivastava, J. Phys. B **21**, 1055 (1988)
28. C. Ma, C.R. Sporleder, R.A. Bonham, Rev. Sci. Instrum. **62**, 909 (1991)
29. P. McCallion, M.B. Shah, H.B. Gilbody, J. Phys. B **25**, 1061 (1992)
30. D.P. Almeida, A.C. Fontes, I.S. Mattos, C.L. Godinho, J. Electron Spectrosc. Relat. Phenomena **67**, 503 (1994)
31. S. Brünken, C. Gerth, B. Kanngießer, T. Luhmann, M. Richter, P. Zimmermann, Phys. Rev. A **65**, 042708 (2002)

32. F. Von Busch, J. Doppelfeld, U. Alkemper, U. Kuetgens, S. Fritzsche, **93**, 127 (1998)
33. U. Alkemper, J. Doppelfeld, F. von Busch, Phys. Rev. A **56**, 2741 (1997)
34. S. Ricz, Á. Kövér, M. Jurvansuu, D. Varga, J. Molnár, S. Aksela, Phys. Rev. A **65**, 042707 (2002)
35. P. Lablanquie, S.-M. Huttula, M. Huttula, L. Andric, J. Palaudoux, J.H.D. Eland, Y. Hikosaka, E. Shigemasa, K. Ito, F. Penent, Phys. Chem. Chem. Phys. **13**, 18355 (2011)
36. P. Lablanquie, L. Andric, J. Palaudoux, U. Becker, M. Braune, J. Viefhaus, J.H.D. Eland, F. Penent, J. Electron Spectrosc. Relat. Phenomena **156-158**, 51 (2007)
37. W.C. Wiley, I.H. McLaren, Rev. Sci. Instrum. **26**, 1150 (1955)
38. http://www.roentdek.com/, RoentDek Handels GmbH (n.d.)
39. L.O. Werme, T. Bergmark, K. Siegbahn, Physica Scripta **8**, 149 (1973)
40. W. Lotz, J. Opt. Soc. Am. **58**, 915 (1968)
41. F.P. Larkins, J. Phys. B **4**, 14 (1971)
42. J.A.R. Samson, W.C. Stolte, Z.X. He, J.N. Cutler, D. Hansen, Phys. Rev. A **54**, 2099 (1996)
43. T. Kylli, H. Aksela, O.-P. Sairanen, A. Hiltunen, S. Aksela, J. Phys. B **30**, 3647 (1997)
44. M.Y. Amusia, M.Y. Kuchiev, S.A. Sheinerman, S.I. Sheftel, J. Phys. B **10**, L535 (1977)
45. F. Von Busch, U. Kuetgens, J. Doppelfeld, S. Fritzsche, Phys. Rev. A **59**, 2030 (1999)
46. A. Hiltunen, T. Kylli, J. Mursu, O.-P. Sairanen, H. Aksela, S. Aksela, J. Electron Spectrosc. Relat. Phenomena **87**, 203 (1998)